Acta of Bioengineering and Biomechanics
Vol. 24, No. 4, 2022

Original paper
DOI: 10.37190/ABB-02208-2023-04

Influence of cross-linking time on physico-chemical and mechanical properties of bulk poly(glycerol sebacate)

PAWEŁ PISZKO*, BARTŁOMIEJ KRYSZAK, KONRAD SZUSTAKIEWICZ

Department of Polymer Engineering and Technology, Faculty of Chemistry,
Wrocław University of Science and Technology (WUST), Wrocław, Poland.

In the presented study, a PGS prepolymer (pPGS) was synthesized utilizing polycondensation technique (equimolar sebacic acid:glycerol ratio, 130 °C, 24 h). Subsequently, the pPGS was thermally cross-linked in vacuum oven in 130 °C for 84 and 168 h. The cylindrical and dumbbell-shaped samples were subjected for physico-chemical and thorough mechanical analysis including tensile and compressive strength evaluation as well as dynamic mechanical thermal analysis (DMTA). The study allowed for the investigation of alteration of PGS properties during cross-linking and decay of elastomeric properties over prolonged cross-linking time. Moreover, a deconvolution in FTIR analysis allowed to glimpse into the hydrogen bonding structure of the materials which weakens during the cross-linking. The obtained results can be utilized during designing PGS-based bulk materials for biomedical application where bearing mechanical loads and tuned chemical character is of vital importance.

Key words: *poly(glycerol sebacate), thermal cross-linking, mechanical properties, DMTA*

1. Introduction

PGS is a polyester that can be obtained in a polycondensation of sebacic acid and glycerol [24], [29]. It has an elastomeric character, potential for structural modification as well as cross-linking (thermal or chemical) [20]. Moreover, it is considered biodegrable [19], [21], [42]. PGS-based systems are thoroughly investigated in literature in the scope of potential tissue engineering application [13], [17], [20], [35], [37] or in drug delivery systems [20], [33], [39] The vast majority of studies include porous materials thin films and fibres, all of which mostly in the composite form [5], [11], [32], [35], [36], [41], [42].

PGS, as a matrix, is regarded as a material that resembles the mechanical and biological properties as well as morphology of soft tissues including retinal, nervous or cartilage [20], [29], [33]. Moreover, in recent years, this polyester has gathered attention as a possible material for hard (bone) tissue engineering, especially when bound with materials enhancing mechanical parameters and/or act as an osteoinductive factor [45]–[47]. This particular scientific interest results from the aforementioned biodegrability, possibility to infiltrate it with apatite ceramics (essential in inducing osteoregenerative potential) [6], [27], [30], [48], lack of cytotoxicity [22], [42], [45] and mechanical properties similar to osteoid tissue and other bone tissue-related structures [23], [47].

The mechanical properties of PGS-based systems vary drastically depending on the synthetic pathway, morphology of the material and addition of more components to the composite blend. Therefore, a thorough understanding of physico-chemical and mechanical behaviour of the polymer matrix itself is a significant matter. Especially taking into consideration the fact that every biomedical application needs particular mechanical, physico-chemical and biological properties [20].

This study regards an influence of thermal cross--linking time on physico-chemical and mechanical

* Corresponding author: Paweł Piszko, Department of Polymer Engineering and Technology, Faculty of Chemistry, Wrocław University of Science and Technology (WUST), Wyb. Wyspiańskiego 27, 50-370 Wrocław, Poland. E-mail: pawel.piszko@pwr.edu.pl
Received: March 2nd, 2023
Accepted for publication: March 30th, 2023

properties of bulk PGS. The tensile and compressive tests are utilized to correlate the alterations in mechanical behaviour with progression in cross-linking. The dynamic mechanical thermal analysis (DMTA) study puts an emphasis on the change in viscoelasticity of the analysed specimens. Viscoelasticity is a trait of particular interest in the polymer indicated for soft tissue engineering or as a matrix for hard tissue engineering. The stress relaxation property of viscoelastic material affects cell behaviour such as cellular remodelling or osteogenic differentiation [15]. The novelty of the presented research covers the mechanical and physico-chemical characterization of bulk PGS matrixes not reported previously.

2. Materials and methods

2.1. Prepolymer (pPGS) synthesis and sample formation

The pPGS prepolymer synthesis was conducted on a Mettler Toledo EasyMax® 102 automated reactor. The process was performed solventless with 1:1 monomer molar ratio. To the reaction vessel, 30 g (0.3258 mol) of glycerol and 65.85 g of sebacic acid was weighted in. The reaction was stirred mechanically and heated to 130 °C until monomers were combined. Then, the process continued for 24 h. After the due time, in order to quench the reaction, the temperature was lowered to 25 °C and the product was kept for further post-processing.

Prepolymer was heated up to 60 °C and subsequently 1,5 mL of pPGS was poured into multi-well custom silicon plates in both cylindrical and tensile stress test specimen shapes (in accordance with ISO-527-2:2012). Afterwards, the samples were subjected for thermal cross-linking in 130 °C for 84 and 168 h under reduced pressure. Graphical presentation of synthesis and sample processing is presented in the Fig. 1.

2.2. Water contact angle (WCA)

WCA measurement was conducted with a PG-X contact angle goniometer (Testing Machines, Inc.). Five measurements were carried out for each specimen with arithmetic average as the result and standard deviation as an error.

2.3. Sol/gel content

Sol content was evaluated with previously reported method, but with change of the solvent from THF to ethanol [10], [18]. Namely, three of each cross-linked PGS cylinders were weighted (W_1) and covered with 20 mL of 96% ethyl alcohol (EtOH) for 24 h. After the due time, samples were dried under vacuum in 40 °C for 24 and another 24 h under atmosphere ambient with air circulation and subsequently weighted (W_2). Sol content (S) was calculated as:

$$S = \frac{W_1 - W_2}{W_1} \times 100\% . \tag{1}$$

From the obtained value gel content (G) was calculated as $G = 100\% - S$.

2.4. Infrared spectroscopy

The FT-IR spectra were registered using a Nicolet iZ10 infrared spectrometer (Thermo Scientific, Waltham, MA, USA) equipped with an ATR attachment. The spectra were registered using 32 scans, resolution of 4 cm^{-1} and spectral range between 4000–550 cm^{-1}. Deconvolution of the peaks was performed using Gaussian function fit and integrated using the Omnic software.

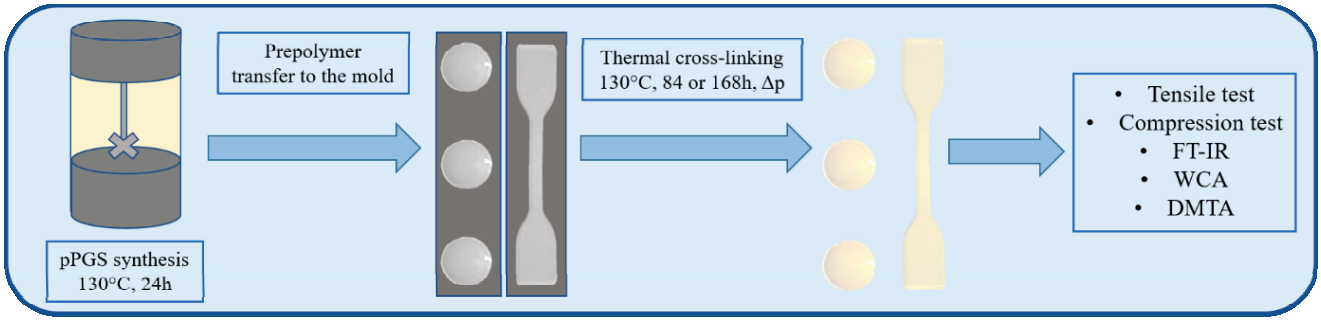

Fig. 1. Graphical schematics of synthesis and formation of bulk PGS samples

2.5. Compressive and tensile strength

Static uniaxial compressive stress evaluation was performed on Instron 5966 universal testing machine with a 10 kN load cell and 1 mm/min compression rate. The cylindrical specimens had dimensions of 15 mm in diameter and 8 mm in height, on average. The measurements were carried out until specimen was damaged or the measurement reached 70% of specimen strain. Obtained stress–strain curves made it possible to determine compressive modulus for both evaluated specimens.

The static tensile strength measurement was performed on the same instrument equipped with 10 kN load cell as well as mechanical wedge grips. The test was carried out with a speed of 10 mm/min until the specimen was broken. For both tensile and compression test, a series of 5 specimens were tested for further data analysis. Young's modulus was calculated as a mean value of linear' fit slope for all samples.

Based on the Young's modulus derived from the tensile test, the cross-linking density (n) was calculated utilizing the formula reported previously [31], [38], [42].

$$n = E_0 / 3RT \,, \tag{2}$$

where:

n – moles of active network chains/unit volume,
E_0 – Young's modulus [Pa],
R – universal gas constant 8.314 [J/(mol·K)],
T – temperature [K].

2.6. DMTA

Dynamic thermomechanical analysis (DMTA) was performed using a DMA/SDTA861e instrument from Mettler Toledo International, Inc. (Greifensee, Switzerland). The tests were carried out in compression mode on cylindrical-shaped samples with a diameter of ~14 mm and a thickness of ~8 mm. First, a number of pre-tests were executed, including the linearity test and the determination of the force offset needed to perform the measurements. The force offset was determined at the level of 1.5 N. Next, the actual viscoelastic measurements were carried out in the temperature range of –50–250 °C with a heating rate of 3 °C/min, at a constant displacement amplitude of 0.2 μm and a frequency of 1 Hz. Finally, frequency sweep tests from 0.1 to 100 Hz were performed in the linear viscoelastic region for a displacement amplitude of 0.2 μm (the same for all samples) at room temperature.

3. Results

3.1. Structural analysis of pPGS

As a polyester, PGS has ester functional groups in its backbone as well as terminal and peripheral carboxylic and hydroxylic groups [13], [23], [33]. During cross-linking, the new covalent ester bonds are formed by condensation reaction between –OH and –COOH groups that could occur both under inter- and intramolecular pathway. The exemplary schematics of formation of a polymeric cross-linked network is presented in Fig. 2D.

The FT-IR spectra registered for prepolymer and cured cylinders are presented in Fig. 2A along with the deconvolution of the carboxylic band (Fig. 2B) and the fit peaks intensity ratio (Fig. 2C). We can outline characteristic bands for PGS which are previously reported in the literature [5], [8], [30]. Namely, broad hydroxyl group (O-H) ~3400 cm^{-1} stretching band, carbonyl (C=O) stretching band ~1730 cm^{-1} and ester stretching band (C-O) ~1160 cm^{-1}. The main distinction between registered spectra is the geometry of the carbonyl peak during the curing process [22]. Method of synthesising PGS utilized in this study results in a polymer with a branching degree of 0.37 [30]. Although, it is not a hyperbranched structure, a study on hyperbranched polyesters [3] reported that the carbonyl band is composed of free and hydrogen-bonded ester carbonyl with alike band morphology. Another reported study on chemically cross-linked poly(butylene sebacate)diol, indicated that deconvolution of the carbonyl peak on the FTIR spectrum was linked to the free and hydrogen-bonded carbonyl [34]. That leads to an observation that during thermal cross-linking of the bulk PGS, a hydrogen bonding steric limitation of ester carbonyl is decreasing. The cause of this could be a cross-linking process resulting in formation of new rigid inter- or intramolecular covalent bonding rather than letting the free polymeric backbones to interact with each other with a hydrogen bonds. The thermal cross-linking also influences the mechanical properties which additionally supports this conclusion. It is reported that both cross-linking and the hydrogen bonding interactions between the –OH groups have a significant effect on elastomeric properties [21], [33]. The plausible mechanistic explanation is depicted in Fig. 2D.

WCA for prepolymer was 48.5°, for the sample cured in 84 h was 74.5°, while after 168 h of curing time, the value increased to 102.7°. Before the

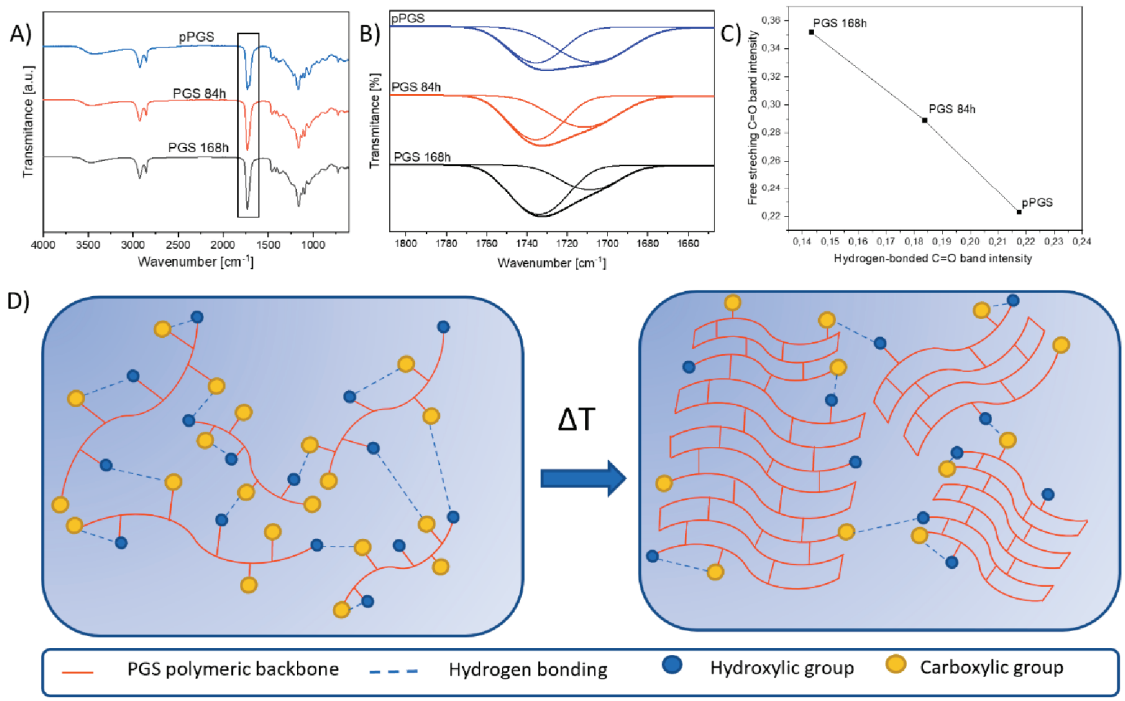

Fig. 2. FT-IR spectra of PGS prepolymer and samples cured at 84 h and 168 h with highlighted carbonyl group area (A), deconvolution of the carbonyl band with Gaussian fit (B), intensity ratio of the free ester carbonyl to the hydrogen bonded one (C) and schematic explanation of the hydrogen bonding decrease (D)

Table 1. Water contact angle measurement, and sol/gel content of the cured PGS samples

Sample	Gel content [%]	Sol content [%]	Water contact angle [°]	Representative WCA drop image
pPGS	0	100	48.5 ± 3.7	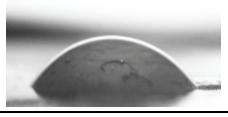
PGS 84 h	81.5 ± 1.5	18.5 ± 9.2	74.5 ± 5.5	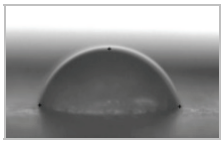
PGS 168 h	97.5 ± 1.6	2.5 ± 2.4	102.7 ± 3.0	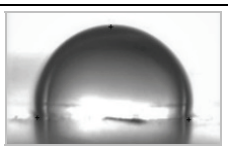

measurement, prepolymer sample was placed on a glass slide and gently heated for 2 minutes in 50 °C in order to distribute the material uniformly on the surface. As reported in the literature, the contact angle for PGS ranges between as low as 30, up to 70–80° [1], [14], [30], [41], [42], which is consistent with the pPGS as well as samples cured over 84 h (Table 1). However, with higher curing time an increase in the WCA value was observed. Therefore, we can observe a gradual weakening in hydrophilic character of the material during cross-linking.

What is more, in Table 1, calculated values of gel and sol content are presented. It is clearly visible that during cross-linking the gel content increases – from 81.5% after 84 h of cross-linking up to 97.5% after 168 h. That means that in the course of the process major part of a soluble in EtOH fraction of prepolymer transforms into a phase non-soluble in EtOH. This conclusion is in line with the study regarding degradation of PGS where the mass of content extracted by EtOH was lower after each cross-linking time interval [31]. The prepolymer was fully soluble

in EtOH. Therefore, its gel content was assumed as 0 and sol content as 100.

3.2. Mechanical properties

The cross-linked PGS specimens were subjected for tensile and compression tests (Fig. 3) as well as DMTA analysis (Fig. 4).

Linear (elastic) and densification regions can be outlined for both tested specimens during the compression (Fig. 3A). Although, for the PGS 168 h sample, the division between both stages is not that sharp. The compressive test of the bulk PGS specimens indicated almost 4-fold increase in compressive modulus (from 0.14 MPa to 0.55 MPa) between PGS 84 h and PGS 168 h samples (Table 2). In literature [36], similar experiments were conducted (the prepolymer syn-

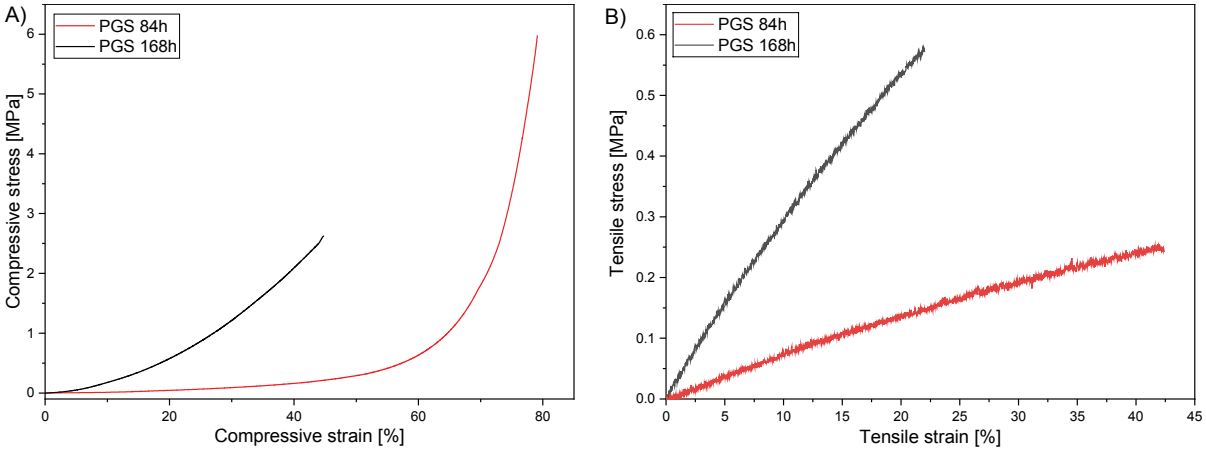

Fig. 3. Compressive (A) and tensile (B) stress–strain curves for cured PGS samples

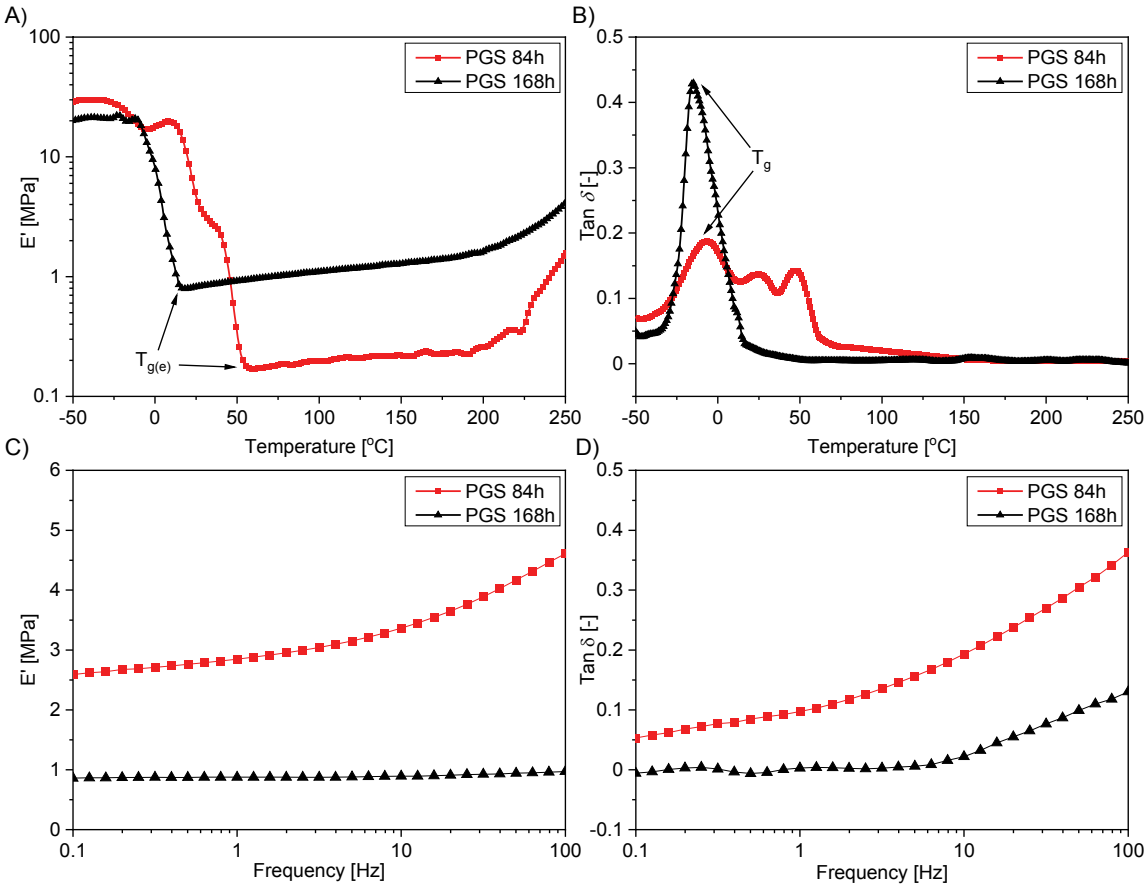

Fig. 4. DMTA results: A, B – Course of changes in the storage modulus and tanδ as a function of temperature, C, D – Storage modulus and tanδ curves obtained during frequency sweep measurements

thesis slightly differed and cross-linking temperature was 120 °C for 96 h), and the obtained compression moduli values were by approximately one order of magnitude lower than the one presented in this study. In case of the other material reported in literature, the bulk PGS which cured for 130 °C in vacuum for 48 h had a compression modulus of 1.67 ± 1.15 MPa [4], which is over 3 times higher than the value for PGS 168 h sample. However, the measurement error for the quoted study was ± 69%. It is vital to understand a critical failure parameters during compression as presented in this study.

The literature reports nonlinear stress–strain behaviour for PGS during tensile strength tests, which is exemplary for soft elastomeric materials [24], [33], [42]. The tensile stress–strain curves obtained in the presented study (Fig. 3B) are in line with this conclusion. Based ondata collected in Table 2, we can observe a 400% increase in tensile modulus (from 0.74 to 2.90 MPa), and 200% increase in ultimate tensile strength (UTS) for the sample cured in 168 h in comparison with the one cured at 84 h. Moreover, in juxtaposition with tensile tests performed in the previously reported studies involving cured thin PGS sheets [24], the UTS was comparable (~0.5 MPa) with PGS sample cured in 168 h. It is worth mentioning that in the referred study, the prepolymer resulted from reduced-pressure polycondensation rather than conventional thermal polycondensation reported in this study. It is vital to recognise that the mechanical properties of PGS polymer are affected by the synthetic pathway and subsequent post-processing (e.g., cross-linking temperature and time [33]) resulting in different degree of polymerization and branching. Moreover, the cross-linking density (n) was calculated based on the Young's modulus derived from the tensile test. It represents the active molecular chains in a volume unit [38]. Its value has risen with the cross-linking time from 99.5 ± 7.3 after 84 h to 389.9 ± 21.7 after 168 h, which remains in the same order of magnitude as for thermally cross-linked PGS reported elsewhere [31]. Taking into consideration increasing values of both gel content and cross-linking density with prolonged curing time, we can correlate those results with an increase of PGS cross-linking degree over processing time.

The DMTA analysis of the samples was performed to determine the mechanical properties of the solid materials as well as the viscoelastic behaviour of the samples during temperature sweep. For both materials, the temperature sweep experiments (Fig. 4A) were performed in the linear viscoelastic regions. In the studies on PGS-based materials, such experiments were usually carried out at low temperatures (from Celsius--negative temperatures to max. 60 °C) in order to record the glass transition [1], [4], [7], [23]. In this study, the focus was also put on the course of the curves at higher temperatures in order to capture the evolution occurring during the thermal cross-linking of the material. If one aims to design a material for tissue engineering, the mechanical parameters are of vital importance.

In Figure 4A, the changes in the storage moduli (E') as a function of temperature are presented. Selected parameters determined from E'(T) curves are listed in the Table 3. At the initial temperature of the measurement (–50 °C), both tested samples are in a glassy state. In both cases the value of the storage modulus reached 20–30 MPa at maximum. At a temperature of about –25 °C, the beginning of the glass transition associated with a significant decrease in the modulus value can be observed. In case of the sample cured in 168 h, this decrease is rapid, while in the case of the

Table 2. Juxtaposition of compressive and tensile moduli, UTS (ultimate tensile strength), tensile strain at break values and stress at 70% strain for compression test derived from the compression and tensile tests

Sample	Compressive modulus [MPa]	Tensile modulus [MPa]	UTS [MPa]	Tensile strain at break [%]	Compressive stress at 70% strain [MPa]
PGS 84 h	0.14 ± 0.01	0.74 ± 0.02	0.25 ± 0.02	43.2 ± 6.6	1.81 ± 0.25
PGS 168 h	0.55 ± 0.03	2.90 ± 0.01	0.56 ± 0.01	22.4 ± 2.9	–

Table 3. Thermomechanical parameters determined from the DMTA curves

Sample	Temperature sweep (Fig. 4A, B)				Frequency sweep (Fig. 4C, D)			
	E' [MPa] at $T_{g(e)}$	E' [MPa] at 250 °C	$T_{g(e)}$ [°C]	T_g [°C]	E' [MPa] at 1 Hz	E' [MPa] at 10 Hz	Tanδ [–] at 1 Hz	Tanδ [–] at 10 Hz
PGS 84 h	0.18	1.57	55.2	–19.7	2.85	3.36	0.097	0.193
PGS 168 h	0.89	4.05	14.2	–25.6	0.88	0.89	0.002	0.022

material cured in 84 h, it is a several-step change, spread over a longer period of time. The nature of the glass transition is well illustrated by the course of the curve of the damping factor (tanδ) in the function of temperature (Fig. 4B).

The differences in the degree of cross-linking of the samples can be clearly seen Fig. 4A. The value of the storage modulus at the temperature of the end of the glass transition ($T_{g(e)}$) is about four times higher for the PGS 164 h sample than for the PGS 84 h one. This is the result of a higher cross-linking density of a sample cured for 164 h. The upward trend of E' moduli is also interesting, indicating further curing of materials, intensified especially above 200 °C.

In the last stage, frequency sweep tests were carried out to study the effect of the oscillation frequency on the viscoelastic behaviour of the tested materials. Figures 4C and 4D show the values of E' and tanδ as a function of the oscillation frequency. In Table 3, the values of the measured parameters for the frequency of 1 and 10 Hz are also compared. As can be seen, the storage modulus is relatively constant in the case of PGS 164 h, however for the PGS 84 h, it tends to increase. The situation with the tanδ parameter is a bit different. As the oscillation increases, it undergoes a significant increase. For the less cross-linked sample (PGS 84 h), this increase is visible throughout the frequency range, whereas for PGS 164 h, the damping factor starts to increase only about the frequency of 10 Hz. An increase in tanδ indicates an increase in the loss modulus and thus the viscous nature of the material. A similar effect was observed in the case of bio-materials based on poly(glycerol sebacate urethane) [1], [6], [9].

4. Discussion

During cross-linking, the intermolecular polycondensation might lead to decrease in amount of peripheral hydroxylic groups. Previously reported plasma surface treatment of the PGS introduced polar groups to the surface which lowered the contact angle and increased the hydrophilicity [41]. Therefore, the proposed explanation of decrease in number of polar (hydrophilic) groups and increase in hydrophobicity after prolonged curing time is plausible. Accessible hydroxyl groups are necessary for further structural modification of PGS such as acrylation [25], [39] or grafting with hexamethylene diisocyanate (HDI) [43] for the sake of chemical or photochemical curing. Nonetheless, this study is focused on thermal curing which does not require further structural modification of PGS.

We can directly correlate the advancement in cross-linking with alteration of tensile and compression properties (i.e., increase in both compressive and tensile moduli). Moreover, the FT-IR analysis (Fig. 2) depicts a gradual decrease in the hydrogen bonding restriction of carbonyl bond which is a direct indication of formation of inter- or intramolecular covalent bonding. The study proposes a plausible mechanistic explanation of presence of hydrogen bonding in the polymer matrix during cross-linking (Fig. 2D). Furthermore, the curing process has an increasing effect on both gel content and cross-linking density. Therefore, it is claimed that a 3D PGS cross-linked network has a decreased elastomeric character as well as more stiffness introduced to the matrix in comparison with semi-crosslinked or prepolymer structures. If one aims to design a material for tissue engineering, the mechanical parameters are important. For example, if the potential implant has higher elastic modulus than the surrounding tissue, it may reduce the mechanostimulation (which is essential in bone tissue regeneration) [15].

When discussing the viscoelastic characteristics of the materials, it is necessary to refer to the properties of the pPGS prepolymer itself. The literature shows that the great challenge is to produce pPGS with a narrow molecular weight distribution. Typically, a product of several fractions with significantly different molecular weights is obtained [28], [44]. This translates into its physicochemical properties – calorimetric studies show even several melting peaks at different temperatures above the glass transition [2], [36], [44] (all these effect often overlap). Returning to the tested materials, for the PGS 84 h sample containing a significant part of the non-crosslinked phase, the effect of the decrease in the E' parameter may be the result of all these phase transformations. Hence, interpreting Fig. 4B, in addition to the maximum at T_g = –19.7 °C related to the glass transition temperature, additional smaller peaks are observed, resulting from the melting of the non-cross-linked fractions. A similar wide and "jagged" glass transition effect visible on the tan$\delta(T)$ curve for less cross-linked samples was demonstrated also in other article [44]. The PGS 164 h sample which is more cross-linked, has a glass transition in a more narrow temperature range and glass transition temperature of T_g = –25.6 °C. The content of the non-cross-linked phase is so small that it does not affect the value of the storage modules during glass transition to a greater extent. The visible effect is visible only at higher temperatures, when cross-linking of the remaining non-cross-linked phase occurs, causing an increase in the value of E' (Fig. 4a).

To sum up, a higher degree of cross-linking makes it possible to obtain materials that are more rigid on the one hand and less susceptible to plastic deformation on the other, which increases their potential in soft tissue engineering for dynamic environments [9].

5. Conclusions

Cross-linking time of PGS is an important factor considering the presented results. It is a variable that gives an overview of change in structural and mechanical parameters over the course of thermal cross-linking. During thermal cross-linking of the PGS matrix we observe a gradual decay in elastomeric character proved by both tensile and compression tests as well as DMTA. During thermal cross-linking over time, an increase of tensile, compressive as well as storage moduli is observed. It gives an indication of increased stiffness of the material as well as its capability of storing energy elastically. Moreover, DMTA was proven as a tool for determination of viscoelastic properties of PGS in various ranges of temperatures and frequencies as well as to observe changes occurring with the progress of cross-linking.

The results are correlated with the presence of hydrogen bonding restricting the carbonyl group on the polymer backbone. Over cross-linking time the effect of the hydrogen bonding is dampened. Therefore, we can assume that the 3D network is being formed, which affects the final properties of the matrix. This structural effect is also confirmed by increase in WCA, caused by cross-linking and subsequent decrease in amount of peripheral polar hydroxylic groups responsible for hydrophilic interactions In the light of presented results, a feasible method of synthesizing a PGS matrix with properties within the showcased parameter range is introduced.

Acknowledgements

The "Multifunctional biologically active composites for applications in bone regenerative medicine" project is carried out within the TEAM-NET program of the Foundation for Polish Science financed by the European Union under the European Regional Development Fund.

Declaration of interests

The authors declare that they have no known competing financial interests or personal relationships that could have appeared to influence the work reported in this paper.

References

[1] AGHAJAN M.H., PANAHI-SARMAD M., ALIKARAMI N., SHOJAEI S., SAEIDI A., KHONAKDAR H.A. et al., *Using solvent-free approach for preparing innovative biopolymer nanocomposites based on PGS/gelatin*, Eur. Polym. J., 2020, 131, 109720.

[2] AYDIN H.M., SALIMI K., RZAYEV Z.M.O., PIŞKIN E., *Microwave-assisted rapid synthesis of poly(glycerol-sebacate) elastomers*, Biomater. Sci., 2013, 1, 5, 503–509.

[3] CALVO-CORREAS T., GABILONDO N., ALONSO-VARONA A., PALOMARES T., CORCUERA M.A., ECEIZA A., *Shape-memory properties of crosslinked biobased polyurethanes*, Eur. Polym. J., 2016, 78, 253–263.

[4] CHEN Q.Z., BISMARCK A., HANSEN U., JUNAID S., TRAN M.Q., HARDING S.E. et al., *Characterisation of a soft elastomer poly(glycerol sebacate) designed to match the mechanical properties of myocardial tissue*, Biomaterials, 2008, 29, 1, 47–57.

[5] DENIZ P., GULER S., ÇELIK E., HOSSEINIAN P., AYDIN H.M., *Use of cyclic strain bioreactor for the upregulation of key tenocyte gene expression on poly(glycerol-sebacate) (PGS) sheets*, Mater Sci. Eng. C., 2020, 106, 110293.

[6] FAKHRI V., JAFARI A., SHAFIEI M.A., EHTESHAMFAR M.V., KHALIGHIYAN S., HOSSEINI H. et al., *Development of physical, mechanical, antibacterial and cell growth properties of poly(glycerol sebacate urethane) (PGSU) with helping of curcumin and hydroxyapatite nanoparticles*, Polym. Chem., 2021, 12, 43, 6263–6282.

[7] FRYDRYCH M., CHEN B., *Fabrication, structure and properties of three-dimensional biodegradable poly(glycerol sebacate urethane) scaffolds*, Polymer, 2017, 122, 159–168.

[8] GADOMSKA-GAJADHUR A., WRZECIONEK M., MATYSZCZAK G., PIĘTOWSKI P., WIĘCŁAW M., RUŚKOWSKI P., *Optimization of poly(glycerol sebacate) Synthesis for Biomedical Purposes with the Design of Experiments*, Org. Process Res. Dev., 2018, 22, 12, 1793–1800.

[9] GUILAK F., RATCLIFFE A., MOW V.C., *Chondrocyte deformation and local tissue strain in articular cartilage: A confocal microscopy study*, J. Orthop. Res., 1996, 13, 3, 410–421.

[10] GUO X.L., LU X.L., DONG D.L., SUN Z.J., *Characterization and optimization of glycerol/sebacate ratio in poly(glycerol-sebacate) elastomer for cell culture application*, J. Biomed. Mater Res. A., 2014, 102, 11, 3903–3907.

[11] HU J., KAI D., YE H., TIAN L., DING X., RAMAKRISHNA S. et al., *Electrospinning of poly(glycerol sebacate)-based nanofibers for nerve tissue engineering*, Mater Sci. Eng. C., 2017, 70, 1089–1094.

[12] JENA K.K., RAJU K.V.S.N., PRATHAB B., AMINABHAVI T.M., *Hyperbranched polyesters: Synthesis, characterization, and molecular simulations*, J. Phys. Chem. B., 2007, 111, 30, 8801–8811.

[13] JIA Y., WANG W., ZHOU X., NIE W., CHEN L., HE C., *Synthesis and characterization of poly(glycerol sebacate)-based elastomeric copolyesters for tissue engineering applications*, Polym. Chem., 2016, 7, 14, 2553–2564.

[14] KERATIVITAYANAN P., GAHARWAR A.K., *Elastomeric and mechanically stiff nanocomposites from poly(glycerol sebacate) and bioactive nanosilicates*, Acta Biomater., 2015, 26, 34–44.

[15] KOONS G.L., DIBA M., MIKOS A.G., *Materials design for bone-tissue engineering*, Nat. Rev. Mater, 2020, 5, 8, 584–603.

[16] LIANG B., SHI Q., XU J., CHAI Y.M., XU J.-G, *Poly (Glycerol Sebacate)-Based Bio-Artificial Multiporous Matrix for Bone Regeneration*, Front. Chem., 2020, 8, 1097.

[17] LIN D., CAI B., WANG L., CAI L., WANG Z., XIE J. et al., *A viscoelastic PEGylated poly(glycerol sebacate)-based bilayer scaffold for cartilage regeneration in full-thickness osteochondral defect*, Biomaterials, 2020, 253, 120095.

[18] LIU Q., TIAN M., DING T., SHI R., FENG Y., ZHANG L. et al., *Preparation and characterization of a thermoplastic poly(glycerol sebacate) elastomer by two-step method*, J. Appl. Polym. Sci., 2007, 103, 3, 1412–1419.

[19] LI Y., HUANG W., COOK W.D., CHEN Q., *A comparative study on poly(xylitol sebacate) and poly(glycerol sebacate): Mechanical properties, biodegradation and cytocompatibility*, Biomed. Mater, 2013, 8, 3.

[20] LOH X.J., ABDUL KARIM A., OWH C., *Poly(glycerol sebacate) biomaterial: synthesis and biomedical applications*, J. Mater Chem. B., 2015, 3, 39, 7641–7652.

[21] MANZANEDO D., ALLEN S.M., *Biorubber (PGS): evaluation of a novel biodegradable elastomer*, 2006, Available at: https://dspace.mit.edu/handle/1721.1/37687 [Accessed: November 23, 2022].

[22] MARTÍN-CABEZUELO R., RODRÍGUEZ-HERNÁNDEZ J.C., VILARIÑO-FELTRER G., VALLÉS-LLUCH A., *Role of curing temperature of poly(glycerol sebacate) substrates on protein-cell interaction and early cell adhesion*, Polymers (Basel), 2021, 13, 3, 1–14.

[23] MA Y., ZHANG W., WANG Z., WANG Z., XI Q., NIU H. et al., *PEGylated poly(glycerol sebacate)-modified calcium phosphate scaffolds with desirable mechanical behavior and enhanced osteogenic capacity*, Acta Biomater., 2016, 44, 110–124.

[24] MATYSZCZAK G., WRZECIONEK M., GADOMSKA-GAJADHUR A., RUŚKOWSKI P., *Kinetics of Polycondensation of Sebacic Acid with Glycerol*, Org. Process Res. Dev., 2020, 24, 6, 1104–1111.

[25] MONEM M., AHMADI Z., FAKHRI V., GOODARZI V., *Preparing and characterization of poly(glycerol-sebacic acid-urethane) (PGSU) nanocomposites: clearing role of unmodified and modified clay nanoparticles*, J. Polym. Res., 2022, 29, 25.

[26] NIJST C.L.E., BRUGGEMAN J.P., KARP J.M., FERREIRA L., ZUMBUEHL A., BETTINGER C.J. et al., *Synthesis and characterization of photocurable elastomers from poly(glycerol-co--sebacate)*, Biomacromolecules, 2007, 8, 10, 3067–3073.

[27] ORLOVSKII V.P., KOMLEV V.S., BARINOV S.M., *Hydroxyapatite and hydroxyapatite-based ceramics*, Inorg. Mater., 2002 38, 10, 973–984.

[28] PERIN G.B., FELISBERTI M.I., *Enzymatic Synthesis of Poly(glycerol sebacate): Kinetics, Chain Growth, and Branching Behavior*, Macromolecules, 2020, 53, 18, 7925–7935.

[29] PISZKO P., KRYSZAK B., PISZKO A., SZUSTAKIEWICZ K., *Brief review on poly(glycerol sebacate) as an emerging polyester in biomedical application: Structure, properties and modifications*, Polim. Med., 2021, 51, 1, 43–50.

[30] PISZKO P., WŁODARCZYK M., ZIELIŃSKA S., GAZIŃSKA M., PŁOCIŃSKI P., RUDNICKA K. et al., *PGS/HAp Microporous Composite Scaffold Obtained in the TIPS-TCL-SL Method: An Innovation for Bone Tissue Engineering*, Int. J. Mol. Sci., 2021, 22, 16, 8587.

[31] POMERANTSEVA I., KREBS N., HART A., NEVILLE C.M., HUANG A.Y., SUNDBACK C.A., *Degradation behavior of poly(glycerol sebacate)*, J. Biomed. Mater Res. A., 2009, 91, 4, 1038–1047.

[32] RAI R., TALLAWI M., BARBANI N., FRATI C., MADEDDU D., CAVALLI S. et al., *Biomimetic poly(glycerol sebacate) (PGS) membranes for cardiac patch application*, Mater Sci. Eng. C., 2013, 33, 7, 3677–3687.

[33] RAI R., TALLAWI M., GRIGORE A., BOCCACCINI A.R., *Synthesis, properties and biomedical applications of poly(glycerol sebacate) (PGS): A review*, Prog. Polym. Sci., 2012, 37, 8, 1051–1078.

[34] ROSTAMIAN M., KALAEE M.R., DEHKORDI S.R., PANAHI--SARMAD M., TIRGAR M., GOODARZI V., *Design and characterization of poly(glycerol-sebacate)-co-poly(caprolactone) (PGS-co-PCL) and its nanocomposites as novel biomaterials: The promising candidate for soft tissue engineering*, Eur. Polym. J., 2020, 138, 109985.

[35] SAUDI A., RAFIENIA M., ZARGAR KHARAZI A., SALEHI H., ZARRABI A., KAREVAN M., *Design and fabrication of poly (glycerol sebacate)-based fibers for neural tissue engineering: Synthesis, electrospinning, and characterization*, Polym. Adv. Technol., 2019, 30, 6, 1427–1440.

[36] SENCADAS V., SADAT S., SILVA D.M., *Mechanical performance of elastomeric PGS scaffolds under dynamic conditions*, J. Mech. Behav. Biomed. Mater, 2020, 102, 103474.

[37] SINGH D., HARDING A.J., ALBADAWI E., BOISSONADE F.M., HAYCOCK J.W., CLAEYSSENS F., *Additive manufactured biodegradable poly(glycerol sebacate methacrylate) nerve guidance conduits*, Acta Biomater., 2018, 78, 48–63.

[38] SPERLING L.H., *Introduction to Physical Polymer Science*, Fourth Ed., 2005.

[39] SUN L., MA Y., NIU H., LIU Y., YUAN Y., LIU C. et al., *Recapitulation of In Situ Endochondral Ossification Using an Injectable Hypoxia-Mimetic Hydrogel*, Adv. Funct. Mater, 2021, 31, 5, 2008515.

[40] SUN Z.J., CHEN C., SUN M.Z., AI C.H., LU X.L., ZHENG Y.F. et al., *The application of poly (glycerol–sebacate) as biodegradable drug carrier*, Biomaterials, 2009, 30, 28, 5209–5214.

[41] THEERATHANAGORN T., THAVORNYUTIKARN B., JANVIKUL W., *Preparation and characterization of plasma-treated porous poly(glycerol sebacate) scaffolds*, Adv. Mat. Res., 2013, 747, 182–185.

[42] WANG Y., AMEER G.A., SHEPPARD B.J., LANGER R., *A tough biodegradable elastomer*, Nat. Biotechnol., 2002, 20, 6, 602–606.

[43] WANG Z., MA Y., WANG Y.X., LIU Y., CHEN K., WU Z. et al., *Urethane-based low-temperature curing, highly-customized and multifunctional poly(glycerol sebacate)-co-poly(ethylene glycol) copolymers*, Acta Biomater., 2018, 71, 279–292.

[44] WU Z., JIN K., WANG L., FAN Y., *Effect of curing time on the mechanical properties of poly(glycerol sebacate)*, J. Appl. Polym. Sci., 2023, 140, 14.

[45] XIAO B., YANG W., LEI D., HUANG J., YIN Y., ZHU Y. et al., *PGS Scaffolds Promote the In Vivo Survival and Directional Differentiation of Bone Marrow Mesenchymal Stem Cells Restoring the Morphology and Function of Wounded Rat Uterus*, Adv. Healthc. Mater, 2019, 8, 5, 1801455

[46] YANG K., ZHANG J., MA X., MA Y., KAN C., MA H. et al., *β-Tricalcium phosphate/poly(glycerol sebacate) scaffolds with robust mechanical property for bone tissue engineering*, Mater. Sci. Eng. C., 2015, 56, 37–47.

[47] ZAKY S.H., LEE K.W., GAO J., JENSEN A., VERDELIS K., WANG Y. et al., *Poly (glycerol sebacate) elastomer supports bone regeneration by its mechanical properties being closer to osteoid tissue rather than to mature bone*, Acta Biomater., 2017, 54, 95–106.

[48] ZHANG P., HONG Z., YU T., CHEN X., JING X., *In vivo mineralization and osteogenesis of nanocomposite scaffold of poly(lactide-co-glycolide) and hydroxyapatite surface-grafted with poly(l-lactide)*, Biomaterials, 2009, 30, 1, 58–70.